


Characteristics of serrated chip formation in high-speed machining of metallic materials

Qibiao Yang¹  · Yin Wu¹ · Dun Liu¹ · Lie Chen¹ · Deyuan Lou¹ · Zhongsheng Zhai¹ · Zhanqiang Liu²

Received: 14 July 2015 / Accepted: 17 December 2015 / Published online: 5 January 2016
© Springer-Verlag London 2016

Abstract A study on the mechanism of serrated chip formation has been carried out. Characterization of serrated chip is performed using geometrical methods, including degree and frequency of segmentation, base angle, and bottom edge. Mechanical characterization such as micro-hardness is also adopted. Experiments of high-speed machining on three metallic materials including Ti6Al4V, hardened 1045 steel, and Al7050 are performed. The chips of the three metallic materials under different cutting speeds are collected during high-speed machining. After polishing, the serrated chip is observed under a digital microscope. The results show that the degree and frequency of segmentation increase with the cutting speed. Al7050 is most sensitive to these parameters. The hardened 1045 steel is similar to the titanium alloy Ti6Al4V. Both the base angle and the vertex angle decrease with the cutting speed. The specific geometry of serrated chip unit under certain cutting speed can be determined by using the geometric characterization parameters. The micro-hardness of the four vertices increases with the increase of cutting speed.

Keywords High-speed machining · Chip characterization · Serrated chip · Chip formation

✉ Qibiao Yang
yangqibiao@mail.hbut.edu.cn

¹ School of Mechanical Engineering, Hubei University of Technology, Wuhan 430068, China

² School of Mechanical Engineering, Shandong University, Jinan 250061, China

1 Introduction

In order to promote the development of manufacturing industry and improve production quality and machining efficiency, reducing processing costs, high-speed machining is widely used in aerospace, automotive, and power generation equipment [1–3]. In comparison with traditional machining conditions, the chip morphology in high-speed machining will emerge great change. Most of the plastic-metal materials will produce continuous chips under traditional machining conditions. However, those under high-speed machining conditions will produce serrated chips [4, 5]. This phenomenon may cause high-frequency fluctuations of cutting force, which can accelerate the wear rate of cutting tool and reduce the machined surface quality and the machining accuracy [6]. Therefore, it is necessary to study the mechanism of serrated chip formation in high-speed machining. Study on the characterization of serrated chip is conducive to a correct understanding of serrated chip formation mechanism in order to develop a reasonable high-speed machining process, improve the efficiency of cutting, ensure the machined surface quality, and reduce tool wear or breakage [7].

Current study on high-speed cutting of the plastic-metal materials is usually focused on the serrated chip formation process, its critical condition, and characterization [8–15]. Based on the literature [8], Turley and Doyle [9] divided the serrated chip formation process into four stages: micro-crack production, shear instability, serrated chip formation, and new serrated chip gradual formation. The critical condition of serrated chip has been studied by several researchers [10–13]. Ignoring the effect of the strain rate hardening, the critical condition is that when the thermal softening effect is about to reach that of the process hardening effect [10]. From the mechanical perspective, it is supposed that the surface unbalance force occurs, and then, the critical condition of adiabatic

shear instability which is the function of the strain, the strain rate, and the cutting temperature was obtained by Lee [11, 12]. Based on the method of linear stability analysis, the critical condition which is the function of the strain, the strain rate, the cutting temperature, and derivatives was obtained by Li [13]. The characterization of serrated chip mainly focused on the geometric shape. By analyzing serrated chip formation process, the analytical solution of unit shear deformation including the shear strain and the shear strain rate was derived by He [14]. As a result of investigation on the serrated chip formation, the analytical solution of adiabatic shear deformation was also obtained [15].

However, the quantitative study on the cutting parameters and its characterization parameters still remains unclear. In order to study the characterization of serrated chip, in this paper, the characterization of serrated chip classified as geometrical and mechanical characterization is studied. The experiment of machining three metallic materials is performed. Some results in the investigation of the cutting speed influence on serrated chip formation characterization are presented.

2 Experimental work

ADAEWOO ACE-V500 vertical machining center was used in the high-speed machining experiment. In this experiment, the Kennametal 90° SN slot milling cutter 4.96164-210 with coated carbide (KC725M) inserts was chosen. The experimental setup is shown in Fig. 1. In order to study the change of the chip characteristics under different lattice types, the three different lattice materials were used, including titanium alloy Ti6Al4V (hexagonal close packed (HCP)), hardened 1045 steel (body-centered cubic lattice (BCC)), and Al7050 (face-centered cubic lattice (FCC)). The chemical composition of the three materials is presented in Tables 1, 2, and 3. Axial depth of cut was 2 mm, and feed per tooth was 0.1 mm/z. In order to obtain a more regular serrated chip, the experiment took different cutting speed ranges due to the different critical cutting speeds of producing the serrated chip in the three materials. Ti6Al4V was machined at the speeds of 100,

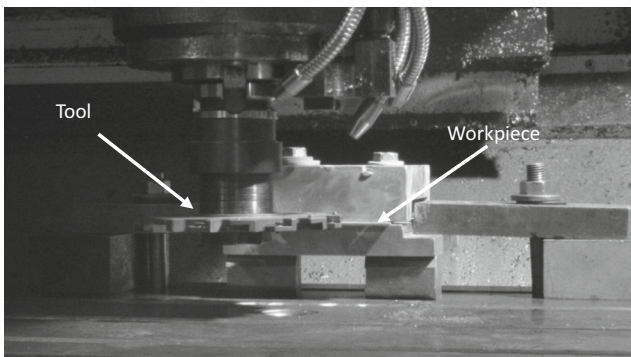


Fig. 1 Experiment setup

Table 1 Chemical composition of Ti6Al4V (wt%)

Ti	C	Fe	N	Al	V	H
Base	0.05	0.09	0.01	6.15	4.40	0.005

300, 500, 700, 1000, and 1500 m/min (six groups), hardened 1045 steel was processed at the speeds of 300, 500, 700, 1000, and 1500 m/min (five groups), and Al7050 was cut at the speeds of 1000, 1500, 2000, 2500, 3000, and 3500 m/min (six groups).

The chips of three materials with different cutting speeds and feeds per tooth have been collected after machining. After inlaying and polishing, the chips were observed under a VHX-600 ESO digital microscope.

3 Characterization of serrated chip

3.1 Geometrical characterization

Compared to continuous chips, serrated chips have two different characteristics: the periodic changes of the chip unit and the nonuniformity variation of the chip thickness. Geometric characterization is to characterize the chip geometry after the serrated chip forming. The change of serrated chip thickness was characterized by the degree of segmentation. As shown in Fig. 2a, the segmentation frequency varies obviously as the cutting speed changing. The shape of serrated chip can be regarded as a trapezoid shown in Fig. 2a. The trapezoid *JILK* is a unit of the serrated chip. The angle between bottom edge *JL* and waist edge *IL* can be called base angle θ_1 . The angle between bottom edge *JL* and waist edge *JK* can be called vertex angle θ_2 . Therefore, the degree of segmentation, the segmentation frequency, the base angle, and the vertex angle can be used for geometric characterization. The geometry shape may be determined by using these geometric characterization parameters.

The geometry measurement of serrated chips is shown in Fig. 2b. Due to ensure measurement data accuracy, it is measured three times to take an average value.

3.1.1 Degree of segmentation

In this paper, the degree of segmentation was defined as Eq. (1) [16]. From the Eq. (1), it is known that the degree of

Table 2 Chemical composition of hardened 1045 steel (wt%)

C	Si	Mn	Cr	Ni	Cu
0.42–0.50	0.17–0.37	0.50–0.80	≤0.25	≤0.30	≤0.25

Table 3 Chemical composition of Al7050 (wt%)

Al	Si	Mn	Cr	Zr	Mg	Cu	Ti	Zn	Fe
Base	0.09	0.08	0.03	0.11	2.00	2.00	0.05	5.7	0.12

segmentation G_s is determined by the maximum height h_1 and the continuous partial height of the serrated chip h_2 . Substituting h_1 and h_2 measured in the experiment test into Eq. (1), the G_s of the three materials under different cutting speeds can be obtained. Through the linear regression method, the quantitative relationship between G_s and the cutting speed can be obtained shown in Fig. 3. It can be found that G_s increases with the increasing of cutting speed. After the calculation, the expression between G_s and the cutting speed is obtained as shown in Eq. (2). From Eq. (2), it can be found that the aluminum alloy 7050 is the most sensitive to G_s , and the hardened 1045 steel is similar to the titanium alloy Ti6Al4V.

$$G_s = 1 - \frac{h_2}{h_1} \tag{1}$$

$$\begin{cases} G_s(Ti6Al4V) = 1.34 \times 10^{-2} \times V^{0.56} \\ G_s(1045) = 2.98 \times 10^{-2} \times V^{0.48} \\ G_s(Al7050) = 1.57 \times 10^{-4} \times V^{1.07} \end{cases} \tag{2}$$

3.1.2 Segmentation frequency

Segmentation frequency can be defined as the number of the serrated chip segment per unit time. Based on the serrated chip formation of plastic-metal materials,

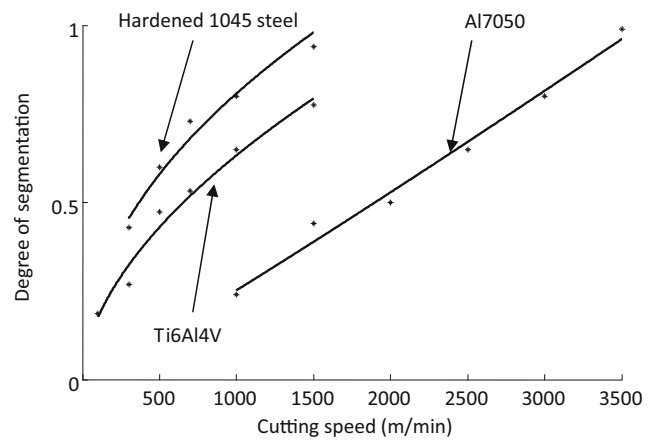


Fig. 3 Changes of the degree of segmentation under different cutting speeds

segmentation frequency can be represented as shown in Eq. (3).

$$f = \frac{V \sin \varphi}{d} \tag{3}$$

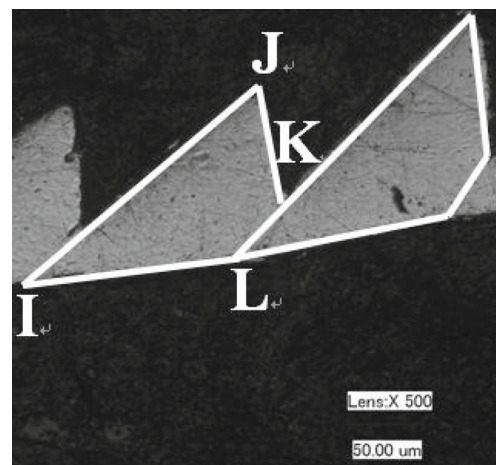
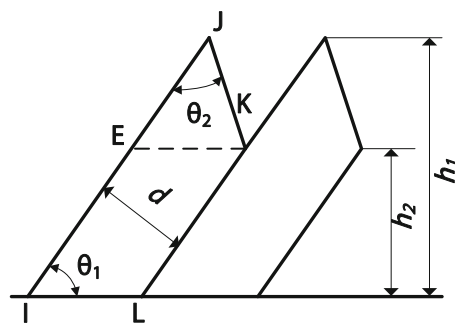
Ignoring the influence of rotation during the serrated chip formation, the quantitative relationship between the shear angle φ , the base angle θ_1 , and the rake angle γ_0 can be expressed as Eq. (4).

$$\frac{\pi}{2} - \varphi + \gamma_0 = \theta_1 \tag{4}$$

where the base angle θ_1 can be measured in the serrated chip unit; therefore, the shear angle φ can be expressed as Eq. (5).

$$\varphi = \frac{\pi}{2} - \theta_1 + \gamma_0 \tag{5}$$

Fig. 2 The geometry and measurement of serrated chips



(a)Geometry of serrated chips (b)Measurement data of serrated chips (Hardened 1045 steel, $V=300\text{m/min}$)

So, substituting Eq. (5) into Eq. (3), the segmentation frequency can be expressed as Eq. (6). In order to obtain the relationship between the segmentation frequency and the cutting speed, the shear band spacing d and the base angle θ_1 of the three different materials have been measured. Through the linear regression method, the quantitative relationship between segmentation frequency f and the cutting speed can be obtained shown in Fig. 4. It can be found that f increases with the increasing of cutting speed. After the calculation, the expression between f and the cutting speed is obtained as shown in Eq. (7). From Eq. (7), it can be found that the aluminum alloy 7050 is the most sensitive to f , the titanium alloy Ti6Al4V followed, and the hardened 1045 steel the least sensitive.

$$f = \frac{V \cos(\theta_1 - \gamma_0)}{d} \tag{6}$$

$$\begin{cases} f(\text{Ti6Al4V}) = 0.66 \times V^{1.25} \\ f(45) = 0.53 \times V^{0.92} \\ f(\text{Al7050}) = 0.30 \times V^{1.4} \end{cases} \tag{7}$$

3.1.3 Base angle and vertex angle

Through measuring the angles in the serrated chip of the experiment above, the base angle and vertex angle of the three materials under different cutting speeds can be obtained shown in Figs. 5 and 6. It can be found that both the base angle and the vertex angle decrease with the increasing of cutting speed. Additionally, the decreasing ratio of Al7050 is much smaller than that of Ti6Al4V and hardened 1045 steel. From the Eq. (5), it is known that the trend of shear angle with the changing of cutting speed is opposite to that of the base angle. This change is similar to that the shear angle changes when generating the continuous chip [1].

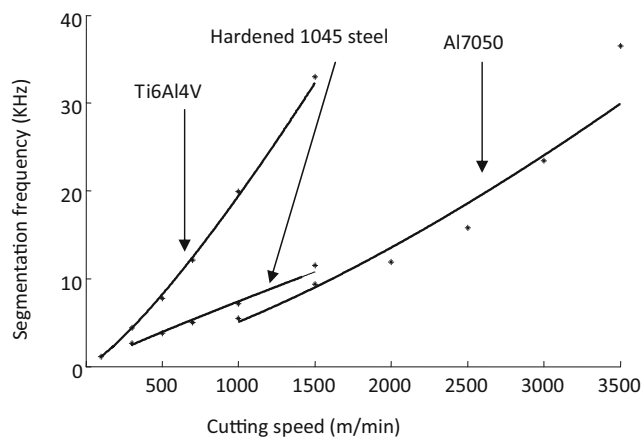


Fig. 4 Changes of the segmentation frequency under different cutting speeds

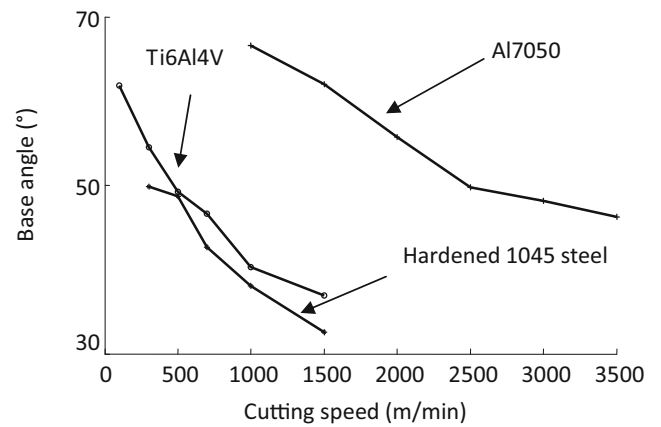


Fig. 5 Changes of the base angle under different cutting speeds

3.1.4 Determination of serrated chip unit

Ignoring the rotation angle due to the action of the torque in the serrated chip formation process, the specific shape can be determined by the geometric characterization parameters above.

As shown in Fig. 2, the size of each side in the trapezoid $JILK$, respectively, is l_{JI} , l_{IL} , l_{LK} , and l_{JK} . The geometric relationship shows that

$$l_{IL} = \frac{d}{\sin \theta_1} \tag{8}$$

Substituting Eq. (6) into Eq. (8), the l_{IL} can be expressed as Eq. (9).

$$l_{IL} = \frac{V \cos(\theta_1 - \gamma_0)}{f \sin \theta_1} \tag{9}$$

By the sine theorem, the Eq. (10) can be obtained in the triangle KJE .

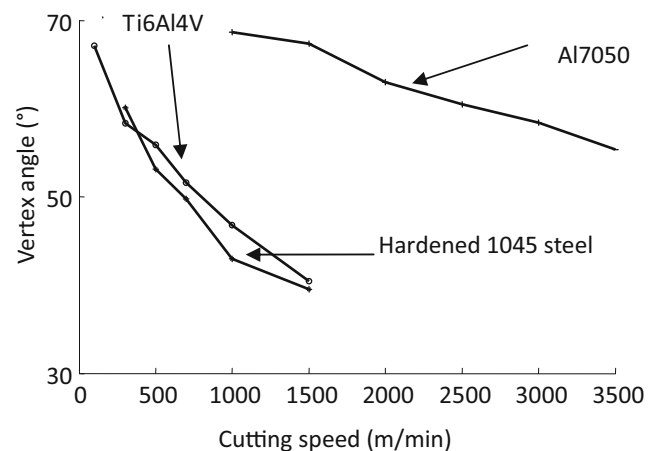


Fig. 6 Changes of the vertex angle under different cutting speeds

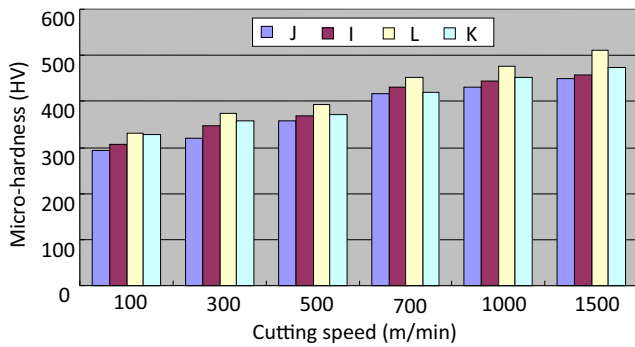


Fig. 7 Changes of micro-hardness under different cutting speeds (Ti6Al4V)

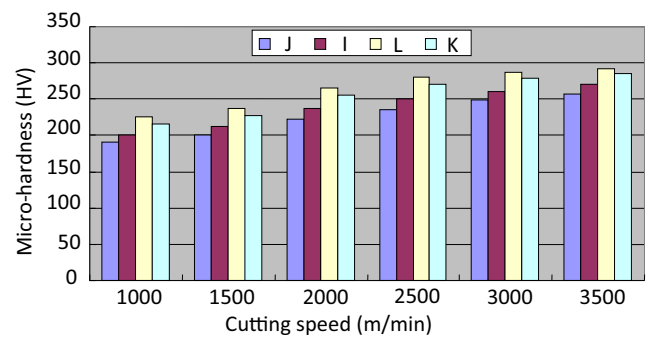


Fig. 9 Changes of micro-hardness under different cutting speeds (Al7050)

$$\frac{l_{KE}}{\sin \theta_2} = \frac{l_{JK}}{\sin \theta_1} = \frac{l_{JE}}{\sin(\pi - \theta_1 - \theta_2)} \tag{10}$$

Therefore, substituting Eq. (9) into Eq. (10), the l_{JK} can be expressed as Eq. (11).

$$l_{JK} = \frac{V \cos(\theta_1 - \gamma_0)}{f \sin \theta_2} \tag{11}$$

From the geometric relations, the degree of segmentation can be expressed as Eq. (12).

$$G_s = \frac{l_{JI} - l_{LK}}{l_{JI}} \tag{12}$$

The relationship between the baseline JI and the topline LK in the trapezoid $JILK$ can be expressed as Eq. (13).

$$l_{JE} = l_{JI} - l_{LK} \tag{13}$$

Therefore, combining Eqs. (10), (12), and (13), the l_{JI} and the l_{LK} can be expressed as follows.

$$l_{JI} = \frac{V \sin(\theta_1 + \theta_2) \cos(\theta_1 - \gamma_0)}{f G_s \sin \theta_1 \sin \theta_2} \tag{14}$$

$$l_{LK} = \frac{V(1 - G_s) \sin(\theta_1 + \theta_2) \cos(\theta_1 - \gamma_0)}{f G_s \sin \theta_1 \sin \theta_2} \tag{15}$$

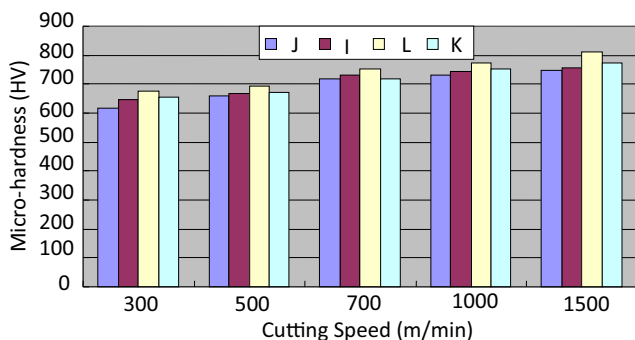


Fig. 8 Changes of micro-hardness under different cutting speeds (hardened 1045 steel)

Combining Eqs. (9), (11), (14), and (15), the size of each side in serrated chip unit can be determined. The specific geometry of serrated chip unit under some cutting speed can be determined by using the geometric characterization parameters above. The size of adiabatic shear band spacing d may determine the rate of serrated chip formation [17, 18]. This conclusion can further reveal the deformation characteristics of the serrated chip, so as to provide a reference for the selection of cutting parameters.

3.2 Mechanical characterization

The mechanical behavior of the workpiece material will be changed due to the large deformation and high temperature during the serrated chip formation. This change may affect the chip morphology, cutting forces, and tool life in high-speed machining. Therefore, the mechanical characterization of serrated chip is proposed. Due to obvious change of the micro-hardness during high-speed machining process, in this paper, the micro-hardness of serrated chip is used to characterize the change of mechanical behavior. Due to inhomogeneous deformation and thin thickness in the serrated chip, it is appropriate to use Vickers hardness in the test.

In order to study the changes in different areas of micro-hardness, the HVS-1000 digital micro-hardness tester is used for hardness testing. In accordance with the vertices J , I , L , and K shown in Fig. 2, the micro-hardness of the serrated chip under different cutting speeds has been measured.

The changes of four vertices under different cutting speeds are respectively shown in Figs. 7, 8, and 9. It is found that micro-hardness of the four vertices increases with the increase of cutting speed in the three histograms. For the same material and in the same cutting speed, the micro-hardness of point L is the highest, that of point I and point K is relatively closer, and that of point J is the minimum.

4 Conclusions

The characterization of serrated chip formation in machining the three different lattice materials is regarded as geometrical characterization and mechanical characterization. The geometrical characterization is characterized by the degree of segmentation, the segmentation frequency, the base angle, and the bottom edge. The mechanical characterization is expressed as the micro-hardness. Through high-speed machining, the three metallic materials Ti6Al4V, hardened 1045 steel, and Al7050, the chips under different conditions have been collected. The conclusions are as follows:

1. The degree of segmentation and the segmentation frequency increase with the increasing of cutting speed. The aluminum alloy 7050 is the most sensitive to them, and the hardened 1045 steel is similar to the titanium alloy Ti6Al4V. Both the base angle and the vertex angle increase with the decreasing of cutting speed.
2. Regarding the serrated chip unit as a trapezoid, the theoretical value of each trapezoid side can be calculated by using the geometrical characterization parameters. Then, the specific geometry of serrated chip unit under some cutting speed can be determined by using the geometric characterization parameters. This may reveal the deformation inhomogeneity of the serrated chip and is then to select cutting parameters in the next step.
3. The micro-hardness of the four vertices increases with the increase of cutting speed. For the same material and in the same cutting speed, the micro-hardness of point *L* is the highest, that of point *I* and point *K* is relatively closer, and that of point *J* is the minimum.

Acknowledgments The authors would like to thank the National Natural Science Foundation of China (Grant Nos. 11204071 and 51405141) and Hubei Provincial Department of Education (Grant Nos. Q20151404 and T201405).

References

1. Ai X (2003) Technology of high speed cutting. National Defense Industrial Press, Beijing
2. Atkins AG (2009) The science and engineering of cutting. Elsevier, Oxford
3. Dandekar CR, Shin YC (2012) Modeling of machining of composite materials: a review. *Int J Mach Tools Manuf* 57:102–121
4. Shaw MC, Vyas A (1993) Chip formation in the machining of hardened steel. *CIRP Ann Manuf Technol* 42:29–33
5. Komanduri R, Brown R (1981) On the mechanical of chip segmentation in machining. *J Eng Ind* 10(3):33–51
6. Smith S, Tlustý J (1997) Current trends in high-speed machining. *J Manuf Sci Eng* 119(4B):664–666
7. Yang Q, Liu Z, Wang B (2012) Characterization of chip formation during machining 1045 steel. *Int J Adv Manuf Technol* 63(9–12): 881–886
8. Davies MA, Chou Y, Evans CJ (1996) On the chip morphology, tool wear and cutting mechanics in finish hard turning. *CIRP Ann Manuf Technol* 45(1):77–82
9. Turley DM, Doyle ED, Ramalingam S (1982) Calculation of shear strains in chip formation in titanium. *Mater Sci Eng* 55(1):45–48
10. Recht R F (1964) Catastrophic thermoplastic shear. *J App Mech*: 189–193
11. Lee D (1984) The nature of chip formation in orthogonal machining. *J Eng Mater Technol* 106(1):9–15
12. Lee D (1985) The effect of cutting speed on chip formation under orthogonal machining. *J Eng Ind* 107:55–63
13. Li G (2009) Prediction of adiabatic shear in high speed machining based on linear perturbation analysis. Dalian University of Technology, doctor degree
14. He N, Lee TC, Lau WS (2002) Assessment of deformation of shear localized chip in high speed machining. *J Mater Process Technol* 129(1–3):101–104
15. Duan CZ, Wang MJ, Pang JZ (2006) A calculational model of shear strain and strain rate within shear band in a serrated chip formed during high speed machining. *J Mater Process Technol* 178(1–3): 274–277
16. Schulz H, Abele E (2001) Materials aspects of saw-tooth chip formation in HSC machining. *CIRP Ann Manuf Technol* 50(1):45–48
17. Yang Q, Liu Z, Shi Z, Wang B (2014) Analytical modeling of adiabatic shear band spacing for serrated chip in high-speed machining. *Int J Adv Manuf Technol* 71(9):1901–1908
18. Wang B, Liu Z (2014) Investigations on the chip formation mechanism and shear localization sensitivity of high-speed machining Ti6Al4V. *Int J Adv Manuf Technol* 75(5):1065–1076